atmosphere

MDPI

Article

Current Status, Trends, and Future Directions in Chilean Air Quality: A Data-Driven Perspective

Kevin Basoa [1,2], Zoë L. Fleming [2,3,*], Manuel A. Leiva [4], Carolina Concha [3] and Camilo Menares [2]

[1] Ministerio del Medio Ambiente, Gobierno de Chile, Santiago 8340515, Chile; kevin.basoa@uchile.cl
[2] Center for Climate and Resilience Research, (CR)2, Santiago 8320000, Chile; cmenares@dgf.uchile.cl
[3] Centro de Investigación en Tecnologías para la Sociedad, Facultad de Ingeniería, Universidad del Desarrollo, Santiago 7610658, Chile; carolina.concha@udd.cl
[4] Departamento de Química, Facultad de Ciencia, Universidad de Chile, Santiago 7800003, Chile; manleiva@uchile.cl
* Correspondence: zfleming@udd.cl

Abstract: Air pollution is one of the main problems facing humanity today. Megacities and large urban areas are pollution hotspots. Measuring pollutants and recording these measurements is key to developing effective strategies to reduce the pollution levels to which people are exposed. However, air quality monitoring presents significant challenges (e.g., investment costs, maintenance), which can lead to limited monitoring equipment. Despite this, Chile has an extensive air quality monitoring network, known as the National Air Quality Information System (SINCA in Spanish). This network has more than 200 monitoring stations that measure, record, and display information on pollution levels in different locations in Chile. In this study, all the information available from the SINCA network was systematized to evaluate the completeness of the records and the current trends of several pollutants in Chile. The main results show that most measurements focus on particulate matter and sulfur dioxide concentrations, and many of the measurement stations are located in the central part of the country (32° S–38° S). However, by splitting the data into five macrozones, one can see the regional air quality characteristics and changes. Furthermore, there are significant data gaps at some monitoring stations, which makes it difficult to elaborate a robust analysis. Regarding pollution levels, a significant decrease is observed for the peak Particulate Matter ($PM_{2.5}$) concentrations, with decreases of nearly 40% compared to concentrations at the beginning of the 2000s. This is consistent with the concentration trends, which show negative trends in most cases.

Keywords: air quality monitoring; Chile; trends; air quality network; pollution

check for updates

Academic Editors: Boris Igor Palella and Evangelos Tolis

Received: 31 March 2025
Revised: 27 May 2025
Accepted: 7 June 2025
Published: 16 June 2025

Citation: Basoa, K.; Fleming, Z.L.; Leiva, M.A.; Concha, C.; Menares, C. Current Status, Trends, and Future Directions in Chilean Air Quality: A Data-Driven Perspective. *Atmosphere* **2025**, *16*, 733. https://doi.org/10.3390/atmos16060733

Copyright: © 2025 by the authors. Licensee MDPI, Basel, Switzerland. This article is an open access article distributed under the terms and conditions of the Creative Commons Attribution (CC BY) license (https://creativecommons.org/licenses/by/4.0/).

1. Introduction

Humans have become the primary drivers of environmental change, substantially altering atmospheric composition and resulting in the urgent issue of air pollution we now face. Air pollution is now one of the foremost environmental and public health risks, associated with respiratory and cardiovascular diseases, premature death, and various forms of cancer. The World Health Organization (WHO) states that ambient air pollution is responsible for approximately 4.2 million premature deaths annually, and an average loss of 2.9 years of Life Expectancy [1] highlights the critical nature of this problem. Vulnerable sectors of the population, such as children, the elderly, and individuals with pre-existing health conditions, are particularly susceptible to the harmful effects of polluted air. The economic burden is substantial, with air pollution costing society over USD 8.1 trillion annually, equivalent to 6.1% of the global GDP [2].

Over the past decade, significant strides have been made in understanding emission sources, atmospheric dynamics, pollutant composition, and the health impacts of air pollution. However, significant challenges and knowledge gaps, for instance, the health effects of co-pollutants, where several pollutants interact in complex ways, are not fully understood. Local variability in atmospheric composition adds further complexity, as concentrations of air pollutants can fluctuate markedly due to meteorological conditions, orography, and human activities. Effective air quality monitoring is essential for successful air pollution management strategies.

Global efforts to monitor and improve air quality include establishing air quality standards, implementing pollution control technologies, and conducting public awareness campaigns. Nonetheless, the United Nations Environment Programme (UNEP) has highlighted that many countries still lack modern frameworks needed for effective air pollution control. Currently, only 61% of countries have at least one government-operated air quality monitoring station that openly shares data, leaving many regions underserved [3].

In Latin America and the Caribbean (LAC), although progress has been made, there is still a need for more ambitious, long-term strategies and effective implementation. This is particularly urgent since LAC is the second most urbanized region in the world, with over 80% of its population living in urban areas and high concentrations in megacities. In 2016, approximately 320,000 premature deaths in the region were attributable to ambient air pollution, with the economic cost of these deaths representing 2.4% of the region's GDP [4]. Official air quality data in LAC is limited, covering only 117 cities across 17 of the 33 countries. Nine countries conduct continuous multi-site monitoring, while eight perform periodic monitoring of a few sites, covering just 30% of the urban population in the region [5]. Persistent challenges include assessing biomass burning impacts, regulating industrial emissions, characterizing urban emissions, and understanding the relationship between air quality and climate change. Additionally, data reliability remains a concern, with many countries lacking robust quality assurance and quality control (QA/QC) systems necessary to support scientific research, policy-making, and public health actions.

At least 60% of Chile's population lives in areas that have $PM_{2.5}$ concentrations that are above the Chilean annual limit values of 20 $\mu g/m^3$ [6]. The death rate from $PM_{2.5}$ exposure in Chile is one of the highest in the region at 230 per million inhabitants [7], exceeding deaths from road traffic. A total of 58% of the whole of Latin America is exposed to pollution over the WHO $PM_{2.5}$ annual average guideline levels of 10 ug/m^3 [8]. According to the 2024 annual IQAir report [9], five of the ten most polluted cities in South America are in Chile, although other cities in the region may have significant pollution levels but lack monitoring capacity.

To understand the regional disparities in air quality across Chile, it is useful to divide the country into macrozones with particular climates (as well as different social issues) that drive the air quality issues. In the northern and central zones, industrial emissions are a major concern, while, in the southern and south-central regions, residential wood burning predominates. Pollution peaks during colder months, when firewood consumption increases and valley topography limits atmospheric dispersion. The southern regions experience severe air pollution, often exacerbated by poverty and inadequate housing [10–12].

Sources of air pollution vary widely across transport, industry, and energy production [13]. In Santiago, the capital of Chile, motor vehicles, industrial sources significantly contribute to $PM_{2.5}$ levels. Technological measures have reduced PM_{10} levels, but NO_2 levels continue to rise due to persistent private vehicle use [14,15]. Ozone pollution in Santiago declined during the 2000s but remains high, driven by the increasing number of vehicles, highlighting the need for targeted ozone pollution management strategies [16,17], especially given the complex nature of being a secondary pollutant. Northern Chile's main

pollution sources include cement plants and soil dust, significantly impacting PM_{10} and $PM_{2.5}$ levels. For instance, in Calama, PM_{10} and $PM_{2.5}$ levels frequently exceed WHO guidelines [18].

Pollution hotspots are highlighted by the transport emission inventory [19] and the Inventario Nacional de Emisiones Antropogénicas (INEMA), which offer higher resolution than global datasets like EDGAR [20]. $PM_{2.5}$ trends have decreased annually by -0.5 $\mu g/m^3$ in Santiago and by as much as -4 $\mu g/m^3$ in Coyhaique in the south [6]. Monitoring of SO_2 levels began in 1993, revealing significant concerns due to emissions from the copper mining industry, urban sources, including high sulphur content in fossil fuels (e.g., gasoline, diesel, coal), and non-regulated power plants [21]. Between 2016 and 2021, Chilean emissions of NOx, NMVOCs, and CO rose by 8%, 17%, and 25%, respectively, according to OECD data [22].

Chile has the largest air quality monitoring network in LAC in terms of number and spatio-temporal coverage. The National Air Quality Information System (SINCA, in Spanish) is an online open-access system that includes data from 224 monitoring stations, many of which also report meteorological data. However, SINCA has significant data gaps, emphasizing the need for improved quality assurance protocols [23]. Reliable datasets are vital for accurate analysis and effective policy design [24]. The first official air quality data were recorded in 1994 and 1995 at five stations managed by the Comisión Nacional del Medio Ambiente (CONAMA, which was replaced in 2010 by the Ministry of the Environment (MMA, in Spanish)).

Pollution Prevention Plans (or Decontamination Plans, known as PDAs in Spanish) can be implemented when an area is declared a non-attainment zone. There are 13 regional Atmospheric Decontamination Plans (PDAs), each tailored to the specific pollution context. Public access to these plans is available at https://ppda.mma.gob.cl/ (accessed on 22 May 2025). They include measures such as emission controls, upgrading technology, and tightening industrial regulations. Key components of these plans include public awareness campaigns and monitoring efforts. Efforts to improve energy efficiency and reduce pollution from residential wood burning include the Heater Replacement Programme (PRC, in Spanish) and building retrofits. Environmental awareness campaigns address cultural barriers to the adoption of cleaner cooking and heating systems. Measures such as a 'green tax' on emissions, EURO VI emission standards for new light-duty vehicles, mandatory emissions testing, low-emission zones, and investment in public transport have been implemented.

There is a recognized need for more comprehensive studies across Chile's regions and pollutant sources. Most air quality research focuses on pollutant concentration monitoring, with limited attention to mitigation strategies [25]. A bibliometric analysis and scoping review offer an in-depth look at the evolution of Chilean air pollution research, highlighting its global relevance and the urgent need for continued research and cooperation [26]. Nearly 60% of studies focus on the central region, 23% on the south, and only 10% on the north [26]. Particulate matter has received the most attention, followed by other criteria pollutants (O_3, SO_2, NOx, CO); research on organic compounds and black carbon remains sparse.

In this study, all the public air quality measurements from the Ministry of Environment (MMA) of Chile, from the SINCA network, were compiled, analysed, and discussed, focusing on hourly resolution data from 1993 to 2024. The aim is to assess the reliability and completeness of this data, ensuring it meets quality assurance and quality control (QA/QC) standards. Differences and trends in pollutant concentrations were examined, particularly for PM_{10}, $PM_{2.5}$, CO, SO_2, NO, NO_2, NOx, and O_3, across various regions of Chile. Additionally, the geographical distribution of monitoring stations was explored in relation to population density and industrial activities. This study is rooted in data-

driven insights in order to provide a comprehensive overview of the present state and ongoing trends. By evaluating existing monitoring practices and identifying emerging patterns in pollutant levels, this study aims to derive lessons learned that can inform better decision-making in air quality management and contribute to the development of more effective strategies. These efforts extend beyond Chile to influence air quality management in other countries across the region. Strategic directions are discussed to enhance air quality policies and practices, ensuring they are adaptive and effective in addressing environmental challenges and improving public health outcomes.

2. Materials and Methods

2.1. Geography of Chile and Location of Monitoring Stations

Chile's extensive latitudinal range, complex topography, and diverse climatic conditions create a wide array of air quality challenges throughout the country. To account for this heterogeneity, five macrozones—Norte Grande, Norte Chico, Zona Central, Zona Sur, and Zona Austral—have been defined, reflecting variations in geology, meteorology, and population distribution [27,28]. Each macro-zone presents distinct emission profiles, driven by industrial, urban, and agricultural activities, as well as by the interplay of orography and synoptic-scale circulation patterns.

The Norte Grande, spanning from the Peruvian border to the Copiapó River, encompasses the regions of Arica y Parinacota, Tarapacá, Antofagasta, and Atacama. It is characterized by hyper-arid and desert climates, sparse vegetation, and extensive mining operations, especially copper extraction, which contribute to severe particulate matter (PM_{10} and $PM_{2.5}$) and SO_2 emissions [18,29]. Additional anthropogenic pollution sources arise from industrial coastal areas such as Tocopilla [30]. Together, the four regions of Norte Grande (Table 1) cover more than 260,000 km^2, with a population of approximately 1.7 million inhabitants. The area is monitored by 52 active air quality stations for criteria pollutants, 34 of which operate on an hourly resolution.

Moving southward, the Norte Chico (Coquimbo and Valparaíso regions) exhibits a semi-arid climate, with more frequent rainfall than the far north. Agricultural practices, mining, and power generation facilities contribute significantly to particulate matter (PM_{10}, $PM_{2.5}$) and gaseous pollutants (SO_2, NO_2). Coastal industrial hubs like Quintero-Puchuncaví and Concón have been intensively monitored due to recurring pollution episodes [31,32]. Norte Chico covers roughly 57,000 km^2 and hosts nearly 2.9 million residents, and a total of 43 stations measuring air pollutants, of which 29 record data on an hourly basis.

The Zona Central extends from the Aconcagua River to the Biobío River, including the Metropolitan Region (which contains Santiago), O'Higgins, Maule, Ñuble, and Biobío regions. This area features a Mediterranean climate, with hot, dry summers and cool, rainy winters. It is home to more than half of Chile's population—over 12 million individuals—concentrated primarily in Santiago, where topographic constraints create frequent temperature inversions and limit pollutant dispersion [33]. While much research has focused on Santiago itself, a recent study in the arid Chacabuco province, north of the city, investigated metal content in airborne dust near two tailing ponds and multiple industrial facilities close to residential areas. Using passive sampling methods, this study reported elevated concentrations of metals in dust deposits [34]. Emissions stem from vehicular traffic, industrial activities, and residential wood burning during the colder months, especially in the south of the macrozone. The five regions in Zona Central span ca. 84,000 km^2, with 72 active air quality stations focusing on criteria pollutants, 46 of which meet the criterion of hourly measurements.

The Zona Sur encompasses the Araucanía, Los Ríos, and Los Lagos regions, well known for their abundant rainfall, temperate climate, and extensive agricultural and forestry activities. Emissions include methane, ammonia, and particulates from livestock and crop production, while residential wood combustion is a primary source of $PM_{2.5}$ in urban centers such as Temuco [24]. This macrozone covers approximately 99,000 km^2 with a combined population of 2.3 million, monitored by 19 active stations, 11 of which provide data on an hourly basis.

Table 1. Number of air quality monitoring stations in each region, number of these with >75% completeness, population, and area of each region. The number in the parentheses indicates the number of stations with any type of measurements (e.g., meteorology, gases, or particulate matter measurements).

Region (from North to South)	Macro-Zone	Total Stations with Air Quality Data	Stations with Over 75% of Data Coverage in 2024	Population (Using 2024 Census)	Area (km^2) INE **
Arica y Parinacota	Norte grande	1 (1)	1	244,569	16,873
Tarapacá	Norte grande	1 (1)	1	369,806	42,225
Antofagasta	Norte grande	26 (34)	14	635,416	126,049
Atacama	Norte grande	24 (26)	18	299,180	75,176
Coquimbo	Norte chico	8 (16)	6	832,864	40,579
Valparaíso	Norte chico	35 (38)	23	1,896,053	16,396
Metropolitana	Santiago	13 (14)	10	7,400,741	15,403
O'Higgins	Zona central	13 (14)	7	987,228	16,387
Maule	Zona central	8 (9)	5	1,123,008	30,296
Ñuble	Zona central	6 (6)	2	512,289	13,178
Biobío	Zona central	32 (33)	22	1,613,059	23,890
Araucanía	Zona sur	6 (6)	4	1,010,423	31,842
Los Ríos	Zona sur	5 (7)	2	398,230	18,429
Los Lagos	Zona sur	8 (8)	5	890,284	48,583
Aysén	Zona austral	4 (4)	4	100,745	108,494
Magallanes *	Zona austral	1 (1)	1	166,537	132,297
Total	-	191 (218)	125	18,480,432	756,102

* Chilean Antarctic is not included, ** INE = Instituto Nacional de Estadísticas.

Finally, the Zona Austral extends from the peninsula of Chiloé to Cabo de Hornos at the tip of Latin America, encompassing the Aysén and Magallanes regions. The cool, wet maritime climate and relatively sparse population generally favor good air quality. However, dependence on wood heating in isolated areas can lead to localized pollution episodes, particularly under stable atmospheric conditions [35]. The Zona Austral spans over 240,000 km^2 with a population of around 290,000 inhabitants, with only five air quality stations, all of which measure pollutants on an hourly basis.

Figure 1 shows the station locations, while Table 1 details the number of stations, population, and total area per region. According to official data, 224 stations exist nationwide. In Chile, there is no classification of stations regarding the type of area (e.g., urban, suburban, or rural) or according to the influence of the immediate surroundings (traffic,

industrial, or background) as in Europe and North America. All the stations are in urban or industrial settings—there are no background stations. Of these, 218 monitor air quality parameters, and 191 measure on an hourly resolution. In 2024, only 125 of the hourly-measuring stations reached at least 75% annual data completeness. Comparison across macro-zones reveals that the highest density of monitoring stations—and, consequently, the most comprehensive data coverage—occurs in regions with significant population centers and intensive industrial activities, as exemplified by the Metropolitan Region and coastal industrial belts in Valparaíso and Biobío. This distribution highlights the interplay between demographic pressure, industrial development, and the consequent necessity for more robust air quality assessment networks.

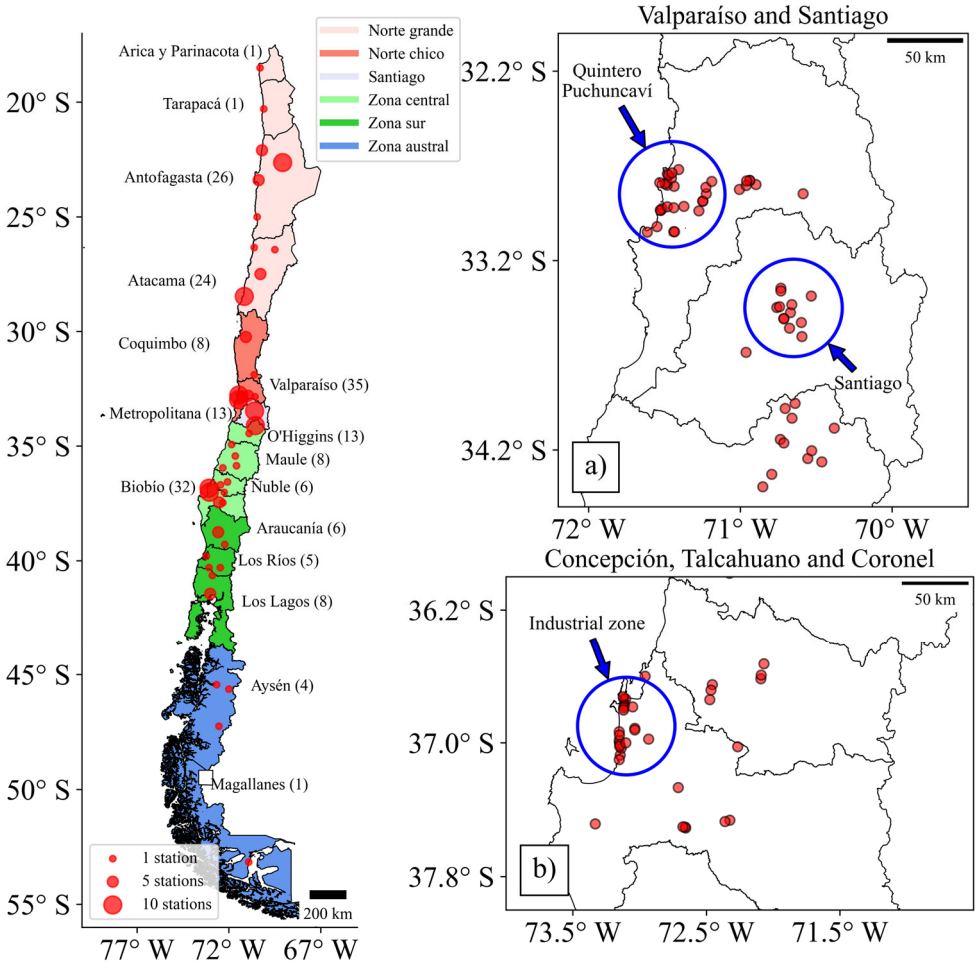


Figure 1. Map of Chile with the 16 political regions (and number of stations by region as per Table 1). The five macrozones are separated by color, with the Metropolitan region (containing Santiago) marked in light blue, despite being part of the Central region. Zoomed images to the right show the detailed distribution of each station for the (**a**) Valparaíso (Quintero-Puchuncaví industrial zone) and the Metropolitan (Santiago) region, and (**b**) the southern city of Concepción and the nearby Coronel (below) and Talcahuano (above) industrial zones.

2.2. The Chilean Air Quality Monitoring Network

The SINCA air quality network, administered by the MMA, provides real-time data on air pollutants and meteorological parameters for numerous Chilean cities. The system operates using the Airviro software platform, developed by the Swedish Meteorological and Hydrological Institute (SMHI), which ensures standardized data management and seamless connectivity (SMHI).

Although stations are strategically located in urban centers exceeding 100,000 inhabitants, areas with high industrial activity also exhibit a higher concentration of monitoring sites (such as Santiago, Quintero-Puchuncaví, and Concepción-Coronel (Figure 1)). The data are available through an interactive online map, employing a color-coded system that distinguishes between multiple levels of pollution alerts, including "alert" and "emergency" statuses (shown in Table S1, in Section S2 of the Supplementary Material).

Each station's dedicated portal provides real-time and historical data, measurement techniques, calibration schedules, and operational details, ensuring traceability and accuracy. Although the MMA has administrative responsibility, maintenance and calibration are typically outsourced to external consultancies, except in Santiago, where the ministry directly supervises operations. Rigorous quality assurance and control protocols guide station performance, encompassing routine maintenance, scheduled calibrations, and systematic data validation.

2.3. Chilean Air Quality Legislation and Compliance

Chilean national air quality standards (ClNAQSs) establish daily and annual standards for various pollutants to control emissions and protect public health. Table S1 (in Section S2 of the Supplementary Materials) compares national standards with the World Health Organization (WHO) guidelines for key pollutants—NO_2, SO_2, CO, O_3, $PM_{2.5}$, and PM_{10}—serving as benchmarks for effective air quality management and policy enforcement. PM_{10} and $PM_{2.5}$ are displayed in $\mu g\ m^{-3,}$ and NO_2, SO_2, CO, and O_3 in ppbv mixing ratio (and CO in ppmv) in all the figures shown in this study, as they appear in these units in all Chilean air quality databases and reports.

Pollutant exceedances are evaluated based on how frequently and for how long threshold values are surpassed. This determines the onset and severity of pollution episodes in accordance with Chilean regulations (see Table S2 in Section S2 of the Supplementary Material). When pollutant concentrations consistently exceed the established thresholds, an environmental emergency is declared, prompting the activation of emission control measures to safeguard public health. In these instances, affected areas are classified as either latent or saturated zones, necessitating the implementation of PDAs to monitor and mitigate pollution levels [28].

2.4. Industrial Zones

Air quality monitoring in Chile is closely associated with industrial activity, as evidenced by the spatial clustering of monitoring stations in major industrial corridors that are often designated as "environmental sacrifice zones", underscoring the disproportionate environmental burden imposed on these areas in terms of public health, ecosystem integrity, and overall quality of life. When these stations are mapped (see Figure 1, right panels), it becomes evident that large-scale industrial operations are clumped together in five main coastal zones. This distribution is not coincidental; rather, it results from environmental regulations that require industrial facilities to monitor their emissions both at source and locally and assess their impacts on air quality. Historically, many of these regions relied on privately operated stations or monitoring networks managed by the Chilean Copper Corporation (CODELCO, in Spanish). However, since 2020, these stations have been integrated into the SINCA national network, thereby improving transparency, regulatory oversight, and public access to environmental information.

These zones support a wide range of industrial activities, including mining, cement production, port operations, fossil fuel power generation, oil refining, copper smelting, and large-scale port operations, that collectively contribute to significant pollution levels. They are also located alongside significant populations residing in close proximity to these

sources of emissions. In Chile, five such sacrifice zones have been officially recognized: Tocopilla, Mejillones, Huasco, Coronel, and Quintero-Puchuncaví. Within these zones, 33 air quality monitoring stations have been deployed to systematically track pollutant concentrations. Figure 2 illustrates the industrial-urban layout and the location of the monitoring stations in Tocopilla (Antofagasta), Huasco (Atacama), Quintero-Puchuncaví (Valparaíso), Coronel (Concepción), Talcahuano (Concepción), and Mejillones (Antofagasta) in the Supplementary Material (Section S3, Figure S1). In these figures, densely monitored industrial regions are depicted alongside human settlements, which are shown in red; population density, derived from the 2017 census, is overlaid in green; the monitoring stations are shown as blue triangles. Where settlements and population data overlap, the population information is superimposed on the red.

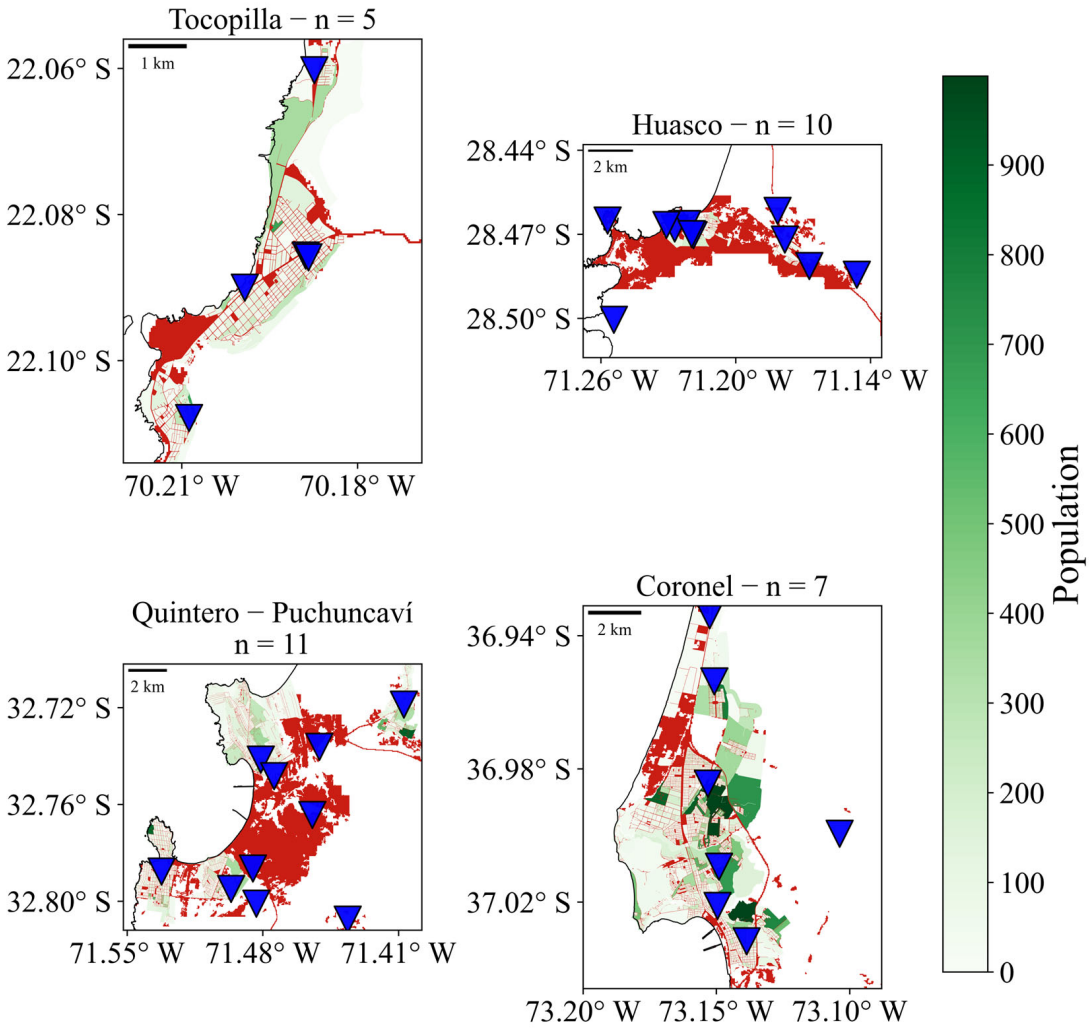


Figure 2. Complementing Figure 1, this figure shows the densely monitored industrial zones (Tocopilla (Antafagasta), Huasco (Atacama), Quintero-Puchuncaví (Valparaiso), and Coronel (Concepción)). Talcahuano and Mejillones are shown in Figure S1 of the Supplementary Materials. Human settlements are shown in red, while the population according to the 2017 census is marked on a scale of green. "n" is the number of monitoring stations (blue triangles). When population and settlements are co-located, population is overlaid over the red. Settlements are adapted from https://chile.mapbiomas.org/ data for 2022 (accessed 1 May 2025).

A particularly striking aspect of these zones is their critical role in Chile's energy production. Of the 28 coal-powered thermoelectric power plants in the country, 27 are located within these industrially burdened areas. In accordance with Chile's commitment

to carbon neutrality under Law 21,455, 10 of these power plants have already been decommissioned, with further closures anticipated. During Chile's presidency of COP25 (2019–2020), the government reaffirmed its strategy to phase out thermoelectric power, improve environmental monitoring, and promote transparency in pollution mitigation efforts and a phase out of all coal-fired thermoelectric plants by 2040 [36].

The environmental impacts in these zones have been extensively documented. Quintero, in particular, has been the focus of numerous studies examining various dimensions of environmental contamination. Recent research includes studies on ambient air quality [31], atmospheric deposition [37], contamination of soils and lake sediments [38], soil pollution [39], rainwater composition [40], pollutant uptake by vegetation [41], and historical trace metal accumulation using dendrochronological methods [42]. Across these studies, consistently elevated concentrations of potentially toxic metals have been reported. Similar trends have been reported near the city of Concepción in Coronel [43] and Tocopilla [30], where industrial emissions have led to substantial accumulations of airborne pollutants and heavy metals in the surrounding environments.

Public awareness of the pollution crisis in these zones increased significantly following the mass hospitalization of school children in Quintero-Puchuncaví in September 2018, an event linked to exposure to unidentified airborne contaminants. This event, along with the widespread social protests of October 2019, which brought longstanding environmental injustices into national focus, prompted authorities to adopt more stringent regulatory measures. Over the past few years, environmental standards have been tightened, monitoring efforts have been expanded, and penalties for pollution violations have increased.

2.5. Statistical Analyses

Considering the extension of the air quality network of Chile and the large records of pollution, the extraction of information could be challenging when a comprehensive and exhaustive analysis is carried out. Thus, automation when downloading information is key for assessing problems related to large volumes of information. All the information from the SINCA network was downloaded using a web scraping algorithm. This was performed for all hourly concentrations for all criteria pollutants (PM_{10}, $PM_{2.5}$, CO, SO_2, O_3, NO_x, NO, and NO_2), between 1993 and 2024, resulting in a dataset of approximately 180 million records. The curated database and corresponding metadata were deposited in the Zenodo data repository.

To perform a comprehensive analysis of the network and assess the current state of the air quality in Chile, several statistical analyses were conducted. Firstly, a completeness analysis of the record from all the monitoring stations was performed in order to assess the spatial and temporal coverage of the network. This analysis considers all publicly available information from the network and aims to show time series consistency and gaps in information. Finally, a statistical test to assess the trend in pollution was performed, focusing on maximum hours of pollution (e.g., rush hour), to better understand if existing policies are addressing pollution issues. A detailed explanation of methods and tools can be found in Section S1 of the Supplementary Material.

3. Results

3.1. Series Completeness and a Glance at Daily Concentrations over the Years

The completeness assessment of the time series considered hourly data from all monitoring stations, identifying 191 stations with robust time series. Figure 3 presents the daily median concentrations of PM_{10} and $PM_{2.5}$—pollutants with the most comprehensive records. The colour scale to the right of the figure illustrates the daily concentrations, ranging from yellow (low concentrations) to dark blue (higher concentrations). A similar

completeness analysis for SO_2 and CO can be found in Figure S2, for O_3 and NOx in Figure S3, and for NO and NO_2 in Figure S4 in Section S3 of the Supplementary Materials.

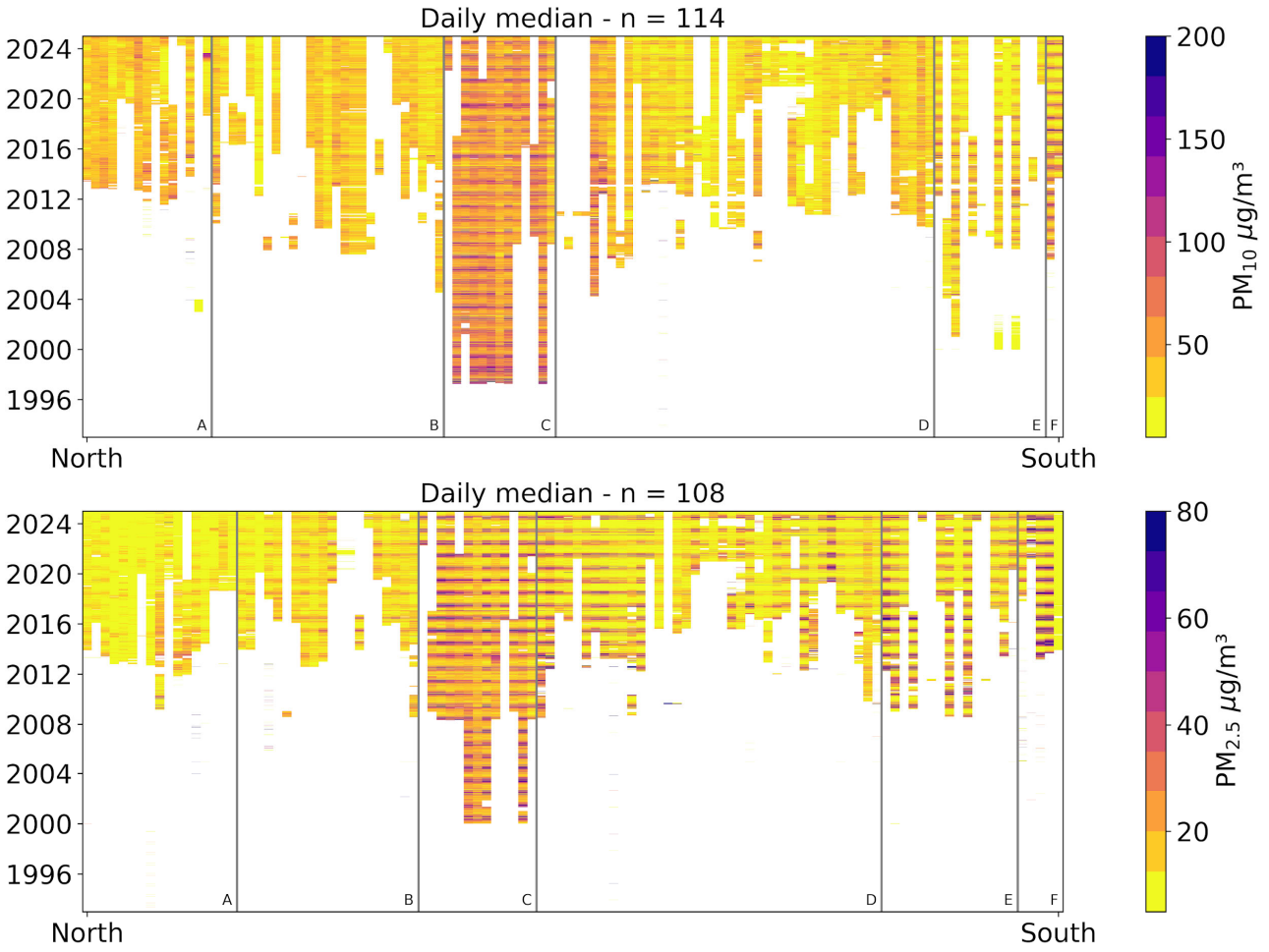


Figure 3. Daily median concentrations of PM_{10} and $PM_{2.5}$ from all monitoring stations with available data. The x-axis is arranged from north (left) to south (right). The number of stations used in each plot is denoted by "n" and letters from A to F indicate the macrozones from Figure 1. A: Norte Grande; B: Norte Chico; C: Santiago; D: Zona Central; D: Zona Sur; F: Zona Austral.

The systematic measurement of SO_2 began in 1993 across various monitoring stations to assess the impact of industrial emissions, particularly in regions characterized by intensive industrial activity in Norte Grande and Norte Chico Macrozones. CO monitoring commenced in Santiago in 1996, while PM_{10} and $PM_{2.5}$ measurements began in 1998 and 2000, respectively, also in the capital. The widespread monitoring of SO_2 reflects Chile's extensive copper smelting operations and the ongoing presence of coal-fired power plants. In northern Chile, certain stations exhibit gaps in SO_2 measurements between 2009 and 2019, whereas, in the central–southern zone, systematic monitoring of SO_2 only started after 2008. Although SO_2 levels were notably high in the earlier years of measurement, some stations continue to report elevated concentrations. PM_{10} levels are persistently high in northern Chile due to arid atmospheric conditions and emissions from mining and power generation. However, annual trends are less discernible in the visualizations shown here. Notably, no SO_2 measurements have been conducted in the Austral region of Chile.

The raw data for PM_{10}, $PM_{2.5}$, and CO exhibit recurring pollution peaks over short time intervals, forming a distinct alternating "striped" pattern indicative of heightened wintertime concentrations. These pollutants are primarily associated with residential heat-

ing, particularly the combustion of firewood. The seasonal increase in $PM_{2.5}$ levels is most pronounced in southern Chile, where winter concentrations frequently exceed 100 $\mu g/m^3$.

The elevated wintertime concentrations of CO and PM_{10} in Santiago prompted the early deployment of monitoring equipment in the capital in 1998, with $PM_{2.5}$ monitoring being implemented a few years later. The concentrations of NO, NO_2, and NOx are strongly correlated with fossil fuel combustion, explaining their high levels in Santiago, where vehicular emissions dominate the pollution profile. O_3 concentrations exhibit a distinct seasonal cycle across all macrozones when a consistent time series is present.

Figures depicting daily, weekly, and annual cycles can be found in Section S3 of the Supplementary Materials further illustrate these patterns, including the observed declines in the SO_2 mixing ratio in Concón (Valparaíso Region, located in the Norte Chico macrozone) and the CO mixing ratios in Parque O'Higgins/Santiago in Figure S5 and Figure S6, respectively. Additionally, persistently high wintertime $PM_{2.5}$ concentrations remain a concern in Coyhaique, as depicted in Figure S7.

3.2. Concentration Cycles

To analyze the temporal variability of air pollutant concentrations and their long-term trends, the 90th percentiles of pollutant concentrations from all Santiago monitoring stations were aggregated and averaged, as illustrated in Figure 4. $PM_{2.5}$ and NO_x exhibit a pronounced bimodal diurnal distribution, with peak concentrations occurring between 06:00 and 10:00 local time in the morning and between 18:00 and 22:00 local time. These peaks are primarily driven by vehicular emissions, atmospheric boundary layer dynamics, and atmospheric stability conditions. The morning peak is more pronounced due to the combined effects of high traffic volumes and temperature inversions that restrict vertical dispersion, leading to an accumulation of pollutants near the surface. The evening peak, although slightly lower in magnitude, is associated with continued emissions under increasingly stable atmospheric conditions as nocturnal cooling intensifies.

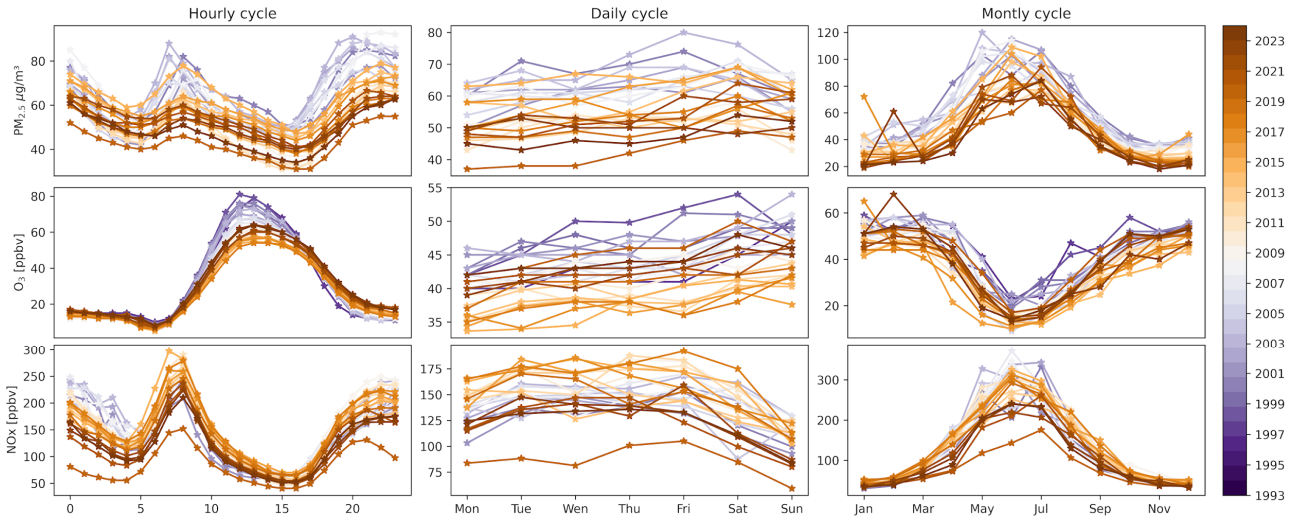


Figure 4. $PM_{2.5}$ (**top**), O_3 (**mid**), and NOx (**bottom**) annual 90th percentile hourly, daily, and monthly concentrations for each year for the average of all monitoring stations in Santiago. For conversion of O_3 ppbv to $\mu g/m^3$ is 1 ppbv = 1.96 $\mu g/m^3$ at 25 °C and 1 atm, and for NOx, 1 ppbv = 1.9125 $\mu g/m^3$.

In contrast, O_3 exhibits a unimodal pattern with maximum concentrations observed between 14:00 and 17:00, coinciding with the period of peak photochemical activity. Tropospheric ozone formation is primarily controlled by photochemical reactions involving nitrogen oxides and volatile organic compounds, with reaction rates strongly dependent on solar radiation intensity. The highest O_3 concentrations are recorded during the warm

season, where elevated temperatures and increased solar irradiance enhance photochemical efficiency, leading to seasonal maxima that exceed winter concentrations by up to 70% in Santiago and even higher in northern regions where solar radiation is more intense [33]. Figure S8 in the Supplementary Materials shows the same hourly, daily, and annual cycles for PM_{10}, CO, and SO_2 for Santiago.

The weekly cycles indicate a systematic reduction in pollutant concentrations on weekends, with the lowest levels typically observed on Sundays. This pattern is particularly evident for NO_x and CO, which are closely linked to vehicular and industrial emissions and show reductions of up to 40% on Sundays compared to weekday levels. $PM_{2.5}$ concentrations follow a similar, though less pronounced, trend influenced by residential wood burning, which is more prevalent at weekends in colder months. O_3 concentrations do not exhibit a significant decrease during weekends; rather, a slight increase is often observed. It is attributed to the reduced availability of NO, which weakens the NO-titration effect and allows O_3 concentrations to remain elevated or even increase in some instances, a phenomenon also observed in other urban areas with high NO_x emissions [15].

Hourly, daily, and monthly cycles for each year of measurements, like those shown for Santiago, were averaged for each of the five macrozones and are shown in Section S3 of the Supplementary Materials in Figures S9 and S10 for PM_{10} and $PM_{2.5}$ and Figures S11–S16 (SO_2, CO, O_3, NOx, NO, and NO_2), and separately for the central zone without Santiago in Figures S17 and S18, exhibiting similar trends in the city as in the five macrozones of Chile. Seasonal variability in pollutant concentrations reveals distinct patterns across pollutants. $PM_{2.5}$ and NO_x reach their highest concentrations during the austral winter months (from May to August), with mean wintertime $PM_{2.5}$ concentrations often exceeding both the annual average limit value of 20 $\mu g/m^3$ and the 24 h limit value of 50 $\mu g/m^3$. This seasonal increase in $PM_{2.5}$ is driven by enhanced emissions from residential heating, particularly wood combustion, coupled with meteorological conditions that favor pollutant accumulation, such as temperature inversions and low atmospheric boundary layer heights, which are most persistent during winter.

The Norte Grande macrozone, characterized by low $PM_{2.5}$ levels and a predominance of PM_{10} from natural sources, such as desert dust and mining activities, presents a different pollution profile (with three apparent peaks during the day) compared to the central and southern regions, where residential heating and vehicular emissions exert a stronger influence on air quality. The annual PM_{10} limit value of 50 $\mu g/m^3$ is surpassed during the peak times of the day in most regions, but the 24 h limit value of 130 $\mu g/m^3$ was rarely reached in recent years.

NO_x concentrations exhibit a similar seasonal trend, with wintertime values elevated due to reduced atmospheric mixing and increased emissions from domestic heating in addition to vehicular and industrial sources. In contrast, O_3 reaches peak concentrations in summer, from December to February, with monthly averages surpassing winter levels by up to 70% in Santiago and even more in the Norte Chico and Zona Central Macrozones, where the solar radiation intensity is higher, favoring increased photochemical activity.

3.3. Industrial Zone Historical Concentrations

Figure 5 shows daily averaged $PM_{2.5}$ and hourly SO_2 concentration timeseries in four industrial zones (Huasco, Quintero-Puchuncaví, Coronel and Talcahuano) along with the Chilean air quality standards as a red dotted line. Analysis of $PM_{2.5}$ concentrations in these industrial zones reveals a lack of significant long-term trends, with neither consistent increases nor decreases observed over the measurement period. However, clear seasonal variations persist, with wintertime concentrations regularly exceeding annual averages by from 40 to 80%, particularly in southern industrial zones where residential biomass

combustion contributes to fine particulate matter pollution. The northern industrial zones of Huasco and Quintero-Puchuncaví exhibit lower $PM_{2.5}$ concentrations relative to their southern counterparts and remain largely in compliance with the Chilean air quality standard of 50 $\mu g/m^3$ for the daily average. In contrast, southern sacrifice zones, such as Coronel and Talcahuano, frequently report exceedances of this threshold, with wintertime daily averages ranging between 55 and 75 $\mu g/m^3$ and episodic peaks surpassing 100 $\mu g/m^3$ during periods of intense atmospheric stability and low ventilation index conditions. These exceedances highlight the compounding effect of industrial emissions and local heating practices, which are particularly relevant in the colder months when biomass combustion for residential heating is prevalent [6].

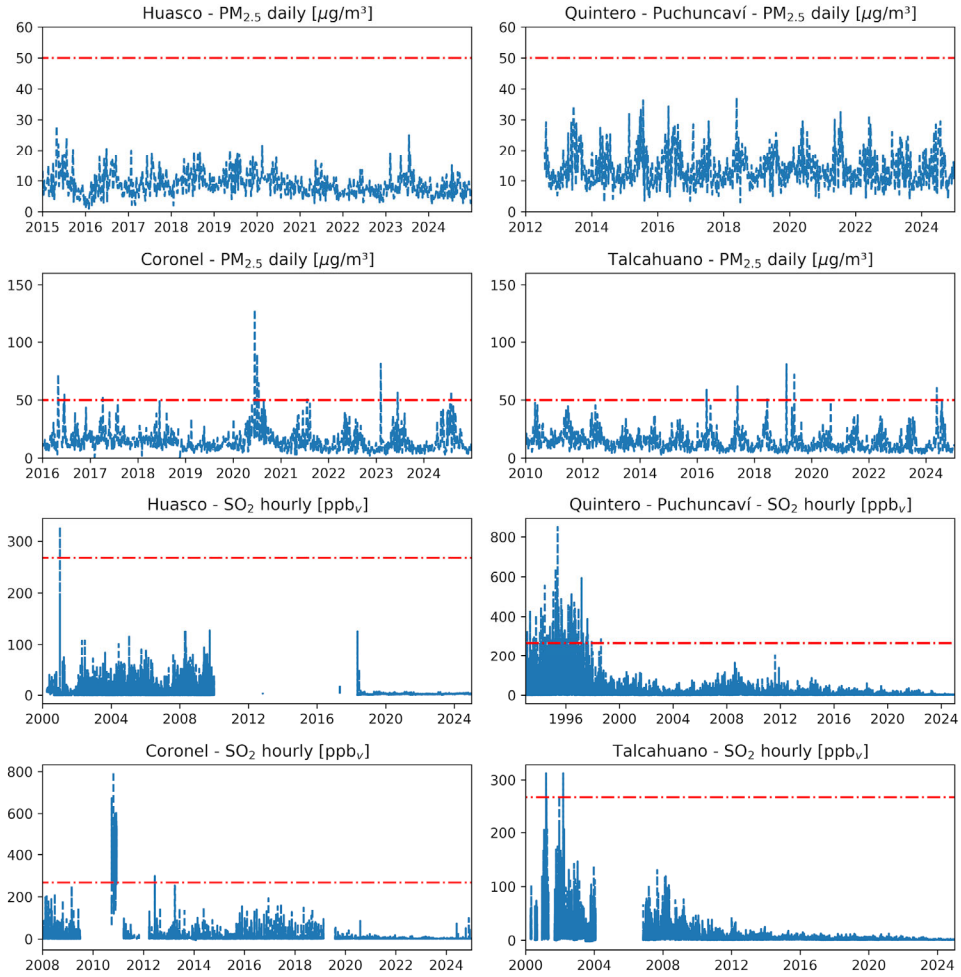


Figure 5. Time series of $PM_{2.5}$ and SO_2 concentrations in four major industrial zones of Chile: Huasco, Quintero-Puchuncaví, Coronel (south of Concepción), and Talcahuano (north of Concepción). The dashed blue lines represent daily average $PM_{2.5}$ concentrations and hourly SO_2 concentrations, while the dashed red lines indicate the Chilean air quality standards of 50 $\mu g/m^3$ for $PM_{2.5}$ (daily average) and 268 ppbv for SO_2 (hourly average). Data points are plotted at intervals of five to enhance readability while preserving the temporal variability of the dataset. For conversion of SO_2 ppbv to $\mu g/m^3$ is 1 ppbv = 2.62 $\mu g/m^3$ at 25 °C and 1 atm.

SO_2 concentrations in industrial zones exhibit a markedly different trend, with a substantial long-term decline observed across all monitored sites. In the early years of measurement, SO_2 concentrations frequently exceeded 100 ppbv, with recurrent hourly spikes surpassing the Chilean regulatory limit of 268 ppbv, particularly in areas with high concentrations of coal-fired power plants and metal smelting facilities. In Quintero-Puchuncaví and Huasco, hourly exceedances of 300–500 ppbv were common in the late 1990s and early

2000s, with some extreme cases reaching 800 ppbv, representing acute pollution episodes with severe implications for respiratory health. Over the past two decades, however, a clear downward trajectory is evident, with annual average SO_2 concentrations declining at a rate of from approximately 5 to 10 ppbv per year, resulting in present-day values consistently below 50 ppbv in all industrial zones. This decline is largely attributable to stricter emissions regulations, the progressive decommissioning of high-sulfur fuel sources, and the implementation of flue gas desulfurization technologies in major industrial facilities [31].

3.4. Trend Analysis

The long-term evolution of pollutant concentrations in all stations was analyzed using high-frequency air quality monitoring data, allowing for the identification of statistically significant trends over the past two decades. Given the spatial variability and diverse industrial activities across these zones, the Mann–Kendall trend analysis [44] was applied to evaluate changes in pollutant levels from 2000 to 2024. This analysis was restricted to stations with a minimum data completeness of 75% to ensure robust statistical interpretations. The focus was placed on the highest pollution periods to assess peak exposure levels, with NO_x and $PM_{2.5}$ trends analyzed during morning rush hours (06:00–10:00) in the cold season (from May to August), while O_3 trends were evaluated in the afternoon (15:00–17:00) during the warmest months (from September to December), when photochemical activity is most intense. The comparison between full-time series and peak-hour trends is presented in Figure 6, demonstrating the consistency of decadal variations.

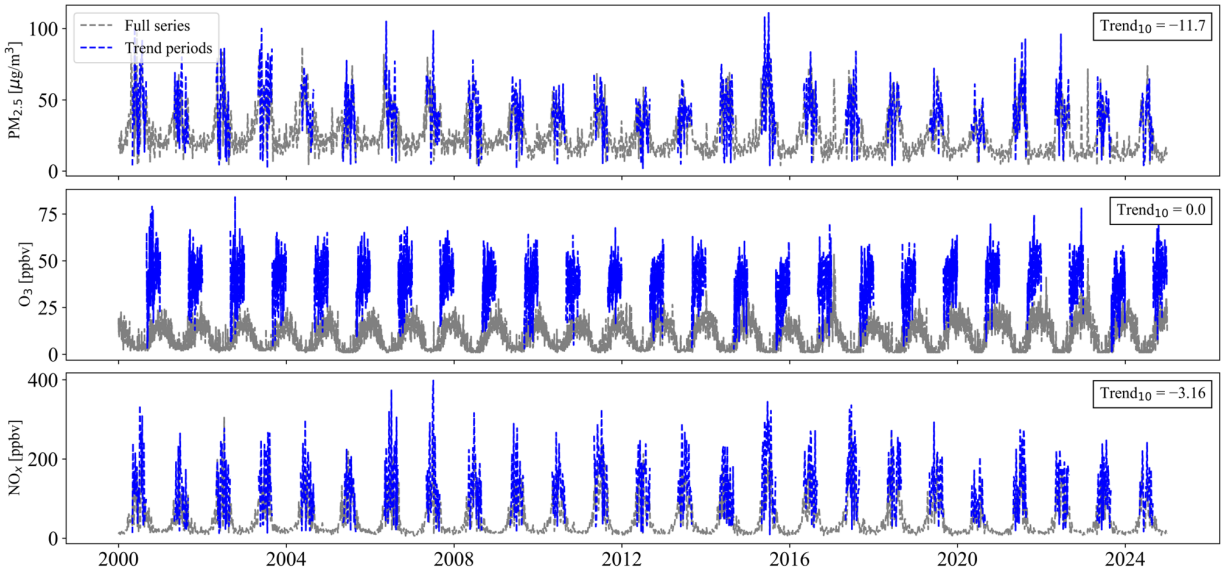


Figure 6. $PM_{2.5}$, O_3, and NO_x concentration time series of all air quality monitoring stations in Santiago between 2000 and 2023. The dashed grey lines represent the full time series of daily average concentrations, while the blue dashed lines highlight the specific time intervals used for trend analysis: 06:00–10:00 for NO_x and $PM_{2.5}$, corresponding to morning rush hour peaks, and 15:00–17:00 for O_3, representing peak photochemical activity during the warm season. The conversion of O_3 ppbv to μg/m^3 is 1 ppbv = 2.62 μg/m^3 at 25 °C and 1 atm, and, for NOx, it is 1 ppbv = 1.9125 μg/m^3.

The numerical results, including trend magnitudes and statistical significance (*p*-values), are summarized in Table 2. $PM_{2.5}$ and NO_x concentrations exhibit a clear downward trend, with an average decadal reduction of 11.7 μg/m^3 per decade for $PM_{2.5}$ and 3.2 ppbv per decade for NO_x, highlighting the effectiveness of emission control strategies targeting vehicular, industrial, and residential heating emissions. However, O_3 mixing ratios do not display statistically significant long-term changes, suggesting that, despite NO_x reductions, the photochemical formation of O_3 has not been sufficiently mitigated.

This behavior is consistent with the complex non-linear relationship between O_3 and its precursors, particularly in VOC-limited urban environments where reductions in NO_x alone may not lead to proportional decreases in O_3 due to weakening of the NO titration effect.

Table 2. Mann–Kendall trend analysis results for monitoring stations in Santiago. Increasing or decreasing trends are highlighted in orange and green if the test meets the *p*-value threshold of 0.05.

Period		**$PM_{2.5}$**			**O_3**			**NOx**	
2000–2024	**Trend**	**μg yr^{-1}**	***p*-Value**	**Trend**	**ppbv yr^{-1}**	***p*-Value**	**Trend**	**ppbv yr^{-1}**	***p*-Value**
Cerrillos I	increasing	4.64	~0	decreasing	−1.13	~0	increasing	5.39	~0
Cerro Navia	no trend	−0.71	0.066	increasing	0.34	~0	decreasing	−4.82	0.002
El Bosque	increasing	0.61	0.016	decreasing	−0.16	0.035	decreasing	−6.61	~0
Independencia	no trend	~0	0.449	decreasing	−0.32	0.010	decreasing	−5.96	~0
La Florida	decreasing	−1.84	-	decreasing	−0.32	0.002	decreasing	−3.77	~0
Las Condes	decreasing	−1.10	-	decreasing	−0.91	~0	decreasing	−0.49	0.050
Parque O'Higgins	decreasing	−3.03	-	decreasing	−0.45	~0	decreasing	−4.77	~0
Pudahuel	no trend	−0.31	0.145	decreasing	−0.27	0.001	no trend	−0.06	0.916
Puente Alto	decreasing	−0.78	~0	increasing	1.20	~0	no trend	−1.42	0.066
Quilicura	no trend	−0.83	0.197						
Quilicura I	increasing	3.58	0.001	decreasing	−2.60	~0	no trend	−1.95	0.572

The spatial distribution of $PM_{2.5}$, O_3, and NO_x trends across Santiago, illustrated in Figure 7, reveals considerable heterogeneity among monitoring stations. $PM_{2.5}$ trends range from +4.64 μg/m^3 per year at Cerrillos I to −3.03 μg/m^3 per year at Parque O'Higgins, reflecting localized variations in emission reductions and meteorological influences. Some stations, including Quilicura and Independencia, show no statistically significant trend, suggesting relatively stable $PM_{2.5}$ levels over time. O_3 concentrations exhibit a predominantly decreasing trend, with reductions of between −0.16 and −2.60 ppbv per year, except at Puente Alto, where an increasing trend of +1.20 ppbv per year is observed, indicating potential shifts in NO_x-to-VOC ratios affecting local O_3 chemistry. NO_x concentrations show a strong decreasing trend, with values ranging from −6.61 ppbv per year at El Bosque to −4.82 ppbv per year at Cerro Navia, reflecting significant reductions in traffic and industrial emissions. However, Cerrillos I presents an anomalous increase of +5.39 ppbv per year, suggesting localized emissions sources or changes in monitoring station siting that may influence recorded values.

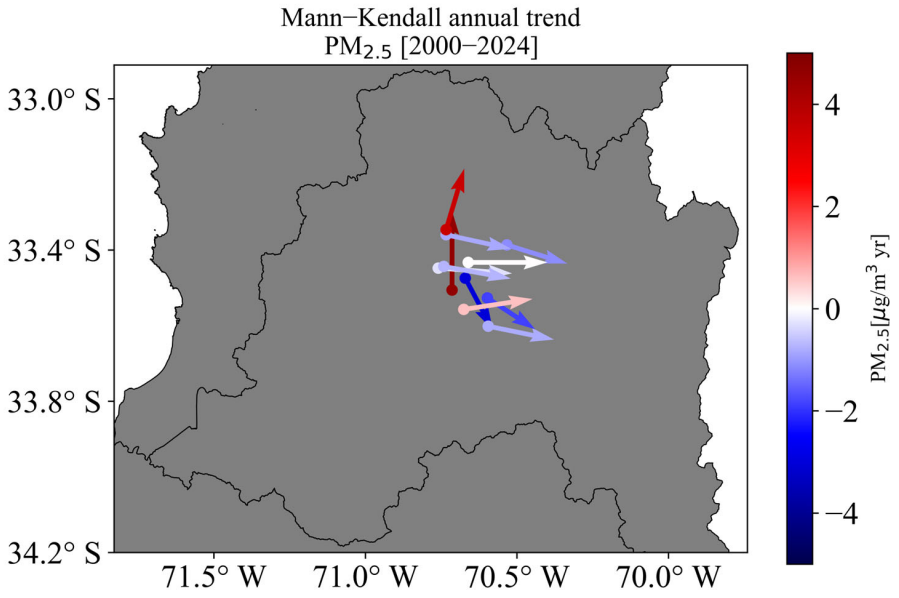


Figure 7. *Cont.*

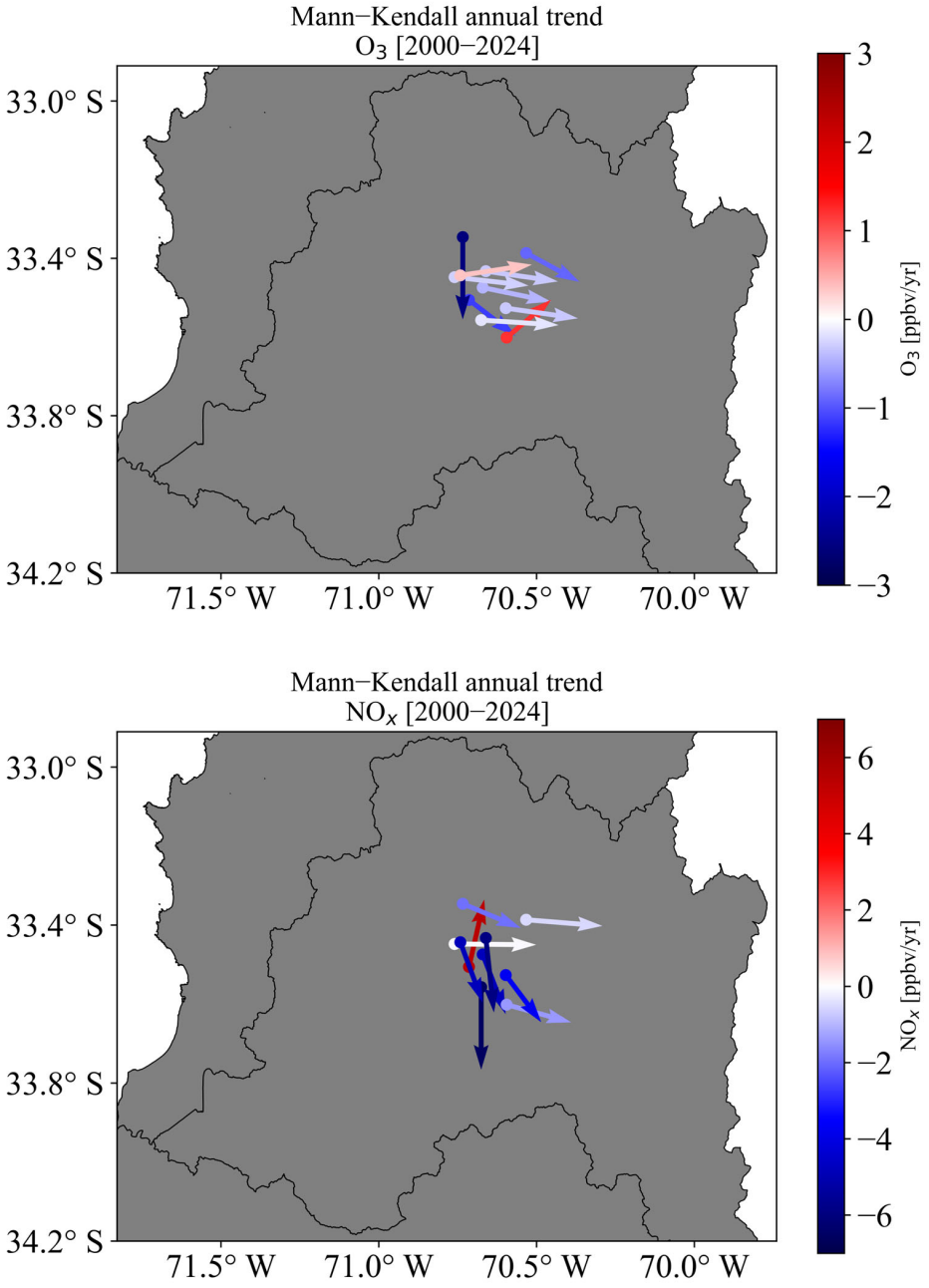


Figure 7. Trend analysis for $PM_{2.5}$, O_3, and NOx for the Santiago monitoring stations. The directions of the arrows indicate increases or decreases in the concentrations. The color intensity indicates the magnitude of the change per year. The solid black line indicates the political regions of Chile.

Anomalies in the long-term dataset are most evident in 2020, when a sharp reduction in traffic activity due to COVID-19 mobility restrictions led to historically low levels of NO_x and $PM_{2.5}$, with concentrations dropping by approximately 30% and 25%, respectively, relative to pre-pandemic averages [33]. This abrupt decrease is consistent with mobility restriction data and reduced fuel consumption reported during lockdown periods. However, an increase in O_3 concentrations was observed despite the decline in NO_x emissions, a response attributed to the nonlinear relationship between O_3 and its precursors, where reduced NO emissions decrease the NO-titration effect, allowing O_3 levels to remain elevated or even increase under conditions of low photochemical destruction. The persistence of elevated O_3 levels despite reduced precursor emissions highlights the need for more targeted photochemical pollution control strategies, particularly in areas with high VOC-

to-NO_x ratios, where O_3 formation is more sensitive to VOC reductions rather than NO_x mitigation alone [15].

National-scale $PM_{2.5}$ and PM_{10} trends from 2000 to 2024, as shown in Figure 8, indicate a consistent decline across most monitoring stations. PM_{10} concentrations exhibit an average annual reduction of 10 $\mu g/m^3$ per year, reflecting the effectiveness of dust suppression and industrial emissions controls, particularly in regions with intensive mining activities. $PM_{2.5}$ concentrations demonstrate a widespread decline, with reductions ranging from -2 to -5 $\mu g/m^3$ per year, reinforcing the impact of stricter vehicle emission standards, cleaner energy transitions, and reduced biomass combustion in residential heating.

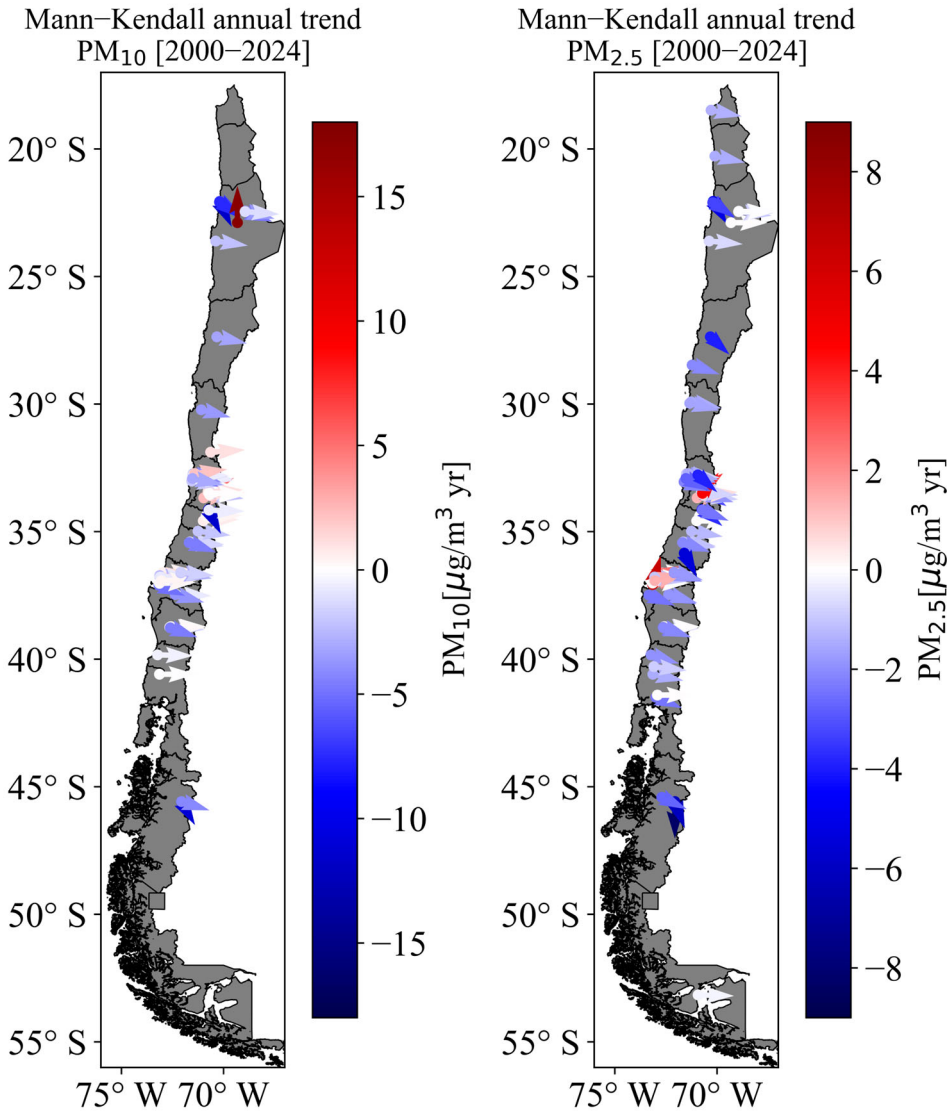


Figure 8. Annual trend analysis for PM_{10} and $PM_{2.5}$ concentrations. The colour indicates the magnitude of change in concentration per year, while arrows indicate the rate of change.

Additional pollutant trend analyses across Chile, detailed in Section S3 of the Supplementary Material (Figures S19–S21), reveal less pronounced trends for SO_2, CO, NO, NO_2, and NO_x. Although most monitoring stations indicate decreasing trends, certain regions in northern and southern Chile exhibit statistically significant increases, potentially linked to localized industrial expansion, urbanization, or regional meteorological effects affecting pollutant dispersion. The full dataset of trend results, including station-specific variations and statistical confidence levels, is presented in Section S4 of the

Supplementary Materials in Tables S3–S10, providing a comprehensive national air quality assessment.

4. Discussion

This comprehensive analysis of Chile's national air quality network—encompassing 271,727 h of data from 191 monitoring stations over a 32-year period (1993–2024)—provides strong quantitative evidence of long-term pollutant trends and spatial heterogeneity across the country. Key pollutants were measured at varying numbers of stations: PM_{10} at 114, $PM_{2.5}$ at 108, SO_2 at 124, CO at 66, O_3 at 74, and NO, NO_2, and NO_x at between 60 and 77 stations. This broad dataset enables robust assessments of data completeness, long-term trends, and cyclic variations on diurnal, weekly, and seasonal scales.

The network's evolution is clearly reflected in the increased station density in areas with high industrial activity and dense urban populations. Notably, five coastal industrial "sacrifice zones" have been targeted with dense monitoring to evaluate compliance with air quality regulations. Despite these improvements, quantitative analysis shows persistent data gaps, particularly in the northern and southern regions, where completeness assessments indicate substantial information deficits and the absence or discontinuity of pollutant measurements.

Statistical evaluations reveal pronounced seasonal cycles: winter months consistently exhibit higher concentrations of PM_{10}, $PM_{2.5}$, CO, and NO_x, primarily driven by increased residential wood burning and stagnant meteorological conditions, while O_3 concentrations reflect intensified photochemical production under higher solar radiation. Diurnal profiles in central and southern regions display clear morning and evening peaks for $PM_{2.5}$ and PM_{10}, with NO_x levels following a bimodal pattern corresponding to rush hour traffic. Additionally, weekly analyses confirm a consistent reduction in pollutant levels during weekends, underscoring the significant influence of anthropogenic emissions.

The spatial and temporal trends observed in SO_2 pollution suggest that regulatory interventions and technological improvements have been effective in mitigating emissions from industrial sources. The transition to lower-sulfur fuels and the implementation of emissions abatement strategies in coal-fired power plants and smelters have contributed to this sustained decrease. However, despite the overall improvement, episodic SO_2 spikes continue to be recorded in certain locations, indicating that localized emission events or fugitive emissions from industrial processes remain a concern. In Coronel and Talcahuano, isolated exceedances of 200–250 ppbv have been documented in recent years, often associated with operational anomalies in industrial plants or adverse meteorological conditions that limit dispersion. While these events are less frequent than in previous decades, they underscore the need for continued emissions monitoring and rapid-response mitigation protocols to prevent acute exposure incidents.

The contrasting trends of $PM_{2.5}$ and SO_2 in Chile's industrial zones highlight the differential effectiveness of pollution control measures. While SO_2 reductions have been substantial and sustained, $PM_{2.5}$ concentrations have remained high, due to the diverse sources contributing to fine particulate matter pollution, including not only industrial activities but also residential heating and secondary aerosol formation processes. Strengthening emission inventories and enhancing real-time air quality management capabilities will be crucial to further improving air quality in Chile's industrial zones and reducing the health burden associated with exposure to fine particulate matter and sulfur dioxide [6,15,31].

Long-term trends indicate a sustained decline in pollutant concentrations over the past two decades, with the most pronounced reductions occurring in the early part of the study period. $PM_{2.5}$ concentrations in Santiago have exhibited an average annual decrease of from approximately 0.5 to 1.0 $\mu g/m^3$ per year, corresponding to a total reduction of nearly 40%

relative to levels observed in the early 2000s and a decrease of 11.7 $\mu g/m^3$ per decade. NO_x concentrations have also declined, with average reductions ranging from 3.2 to 6.6 ppbv per decade, a trend consistent with the implementation of stricter emissions controls and improvements in vehicle emissions standards [15]. The most significant reductions in NO_x concentrations have been observed in central and southern monitoring stations, reflecting the combined effect of fleet renewal, fuel quality improvements, and regional air quality management policies. However, despite these improvements, the overall rate of decrease in NO_x has slowed in recent years, particularly in high-traffic urban areas, suggesting that further mitigation strategies targeting private vehicle use may be necessary to sustain reductions. Unlike primary pollutants, O_3 trends do not show a uniform decline; rather, a mixed behavior is observed, with some stations exhibiting decreasing trends of up to 2 ppbv per year while others, particularly in the southern part of Santiago, show a slight increase, likely attributable to changes in precursor emissions and atmospheric chemistry dynamics.

Across Chile, PM_{10} levels generally decreased at a rate of roughly 10 $\mu g/m^3$ per year, while $PM_{2.5}$ showed annual decreases ranging between 2 and 5 $\mu g/m^3$. There are exceptions in some southern cities where biomass combustion remains a dominant source and has not shown a significant downward trend over the past decade. In industrial zones, while $PM_{2.5}$ concentrations have remained relatively stable (with persistent winter peaks), SO_2 levels have sharply declined from frequent episodic values exceeding 100 ppb and spikes above the 268 ppbv regulatory threshold to sustained concentrations below 50 ppb in recent years. This marked reduction in SO_2 is a quantitative testament to the effectiveness of rigorous industrial emission control policies. However, episodic spikes in SO_2 continue to be recorded, highlighting the need for continued monitoring of short-term emissions events. The spatial distribution of monitoring stations and pollutant trends across Chile underscores the importance of region-specific mitigation strategies, as air quality challenges vary significantly across climatic and socio-economic contexts.

These quantitative findings highlight both the progress achieved and the challenges that remain. While improvements in pollutant levels—driven by decontamination plans, stricter emission standards, improved fuel standards, public transportation policies, and cleaner energy policies—are evident, targeted efforts are still needed in regions reliant on wood combustion and in industrial hotspots with intermittent pollution spikes. The data strongly advocate for enhanced spatial coverage, improved quality assurance protocols, and continued investment in air quality management strategies in order to improve public health outcomes.

5. Conclusions

This study delivers a comprehensive long-term evaluation of air pollution in Chile, analyzing hourly observations of $PM_{2.5}$, PM_{10}, SO_2, NO, NO_2, NO_x, CO, and O_3 from 191 monitoring stations between 1993 and 2024. A key strength lies in the spatial disaggregation by five macrozones—Norte Grande, Norte Chico, Zona Central, Zona Sur, and Zona Austral—capturing regional characteristics shaped by emissions sources, topography, and climate. SO_2 concentrations have declined significantly in industrial zones within the Norte Grande and Norte Chico (from -5 to -10 ppbv per year) Macrozones, driven by fuel transitions and emissions controls. PM_{10} levels have dropped by 8–12 $\mu g/m^3$ annually across much of the country, yet remain high in northern regions due to mining and desert dust. $PM_{2.5}$ has improved markedly in Santiago (-11.7 $\mu g/m^3$ per decade), but reductions in the Zona Sur and Austral are modest (~0.3 $\mu g/m^3$ annually), where residential wood combustion under stagnant meteorological conditions sustains winter peaks above 100 $\mu g/m^3$. CO and NO_x trends are negative across all macrozones, with

the strongest reductions in the central zone, aligning with technological improvements in transport and policy enforcement.

Ozone (O_3) trends reveal spatial heterogeneity: decreases of up to 2 ppbv per year are observed in parts of the Zona Central and Norte Chico, while slight increases occur in VOC-limited areas like southern Santiago, where reduced NO titration alters photochemical dynamics. Seasonal and diurnal patterns differ between macrozones: winter peaks in $PM_{2.5}$, CO, and NO_x dominate in the south; O_3 peaks in summer afternoons across the central and northern zones. Although Chile's air quality monitoring network is the most extensive in Latin America, only 125 stations met the 75% data completeness threshold in 2024, with coverage gaps especially in the Zona Austral and Norte Grande.

This study provides a robust, regionally resolved foundation for future air quality management. Policymakers must prioritize targeted interventions for each macrozone—tackling biomass burning in the south, industrial emissions in the north, and secondary pollutant formation in urban centers—while integrating improved QA/QC systems, real-time monitoring, and climate-health co-benefits into adaptive national strategies.

Supplementary Materials: The following supporting information can be downloaded at: https://www.mdpi.com/article/10.3390/atmos16060733/s1, Section S1: Materials and Methods: Software and computational tools [45–53]; Section S2: Chilean Air Quality Limit levels and Event Classifications [54–60]; Section S3: Supplementary Figures; Section S4: Individual Station trends.

Author Contributions: Conceptualization, Z.L.F., K.B. and M.A.L.; methodology, K.B., C.M. and C.C.; software, K.B. and C.M.; validation, K.B.; formal analysis, K.B.; investigation, Z.L.F., K.B. and M.A.L.; resources, K.B., Z.L.F. and M.A.L.; data curation, K.B. and C.C.; writing—original draft preparation, K.B., Z.L.F. and M.A.L.; writing—review and editing, K.B., Z.L.F. and M.A.L.; visualization, K.B., C.C. and Z.L.F.; supervision, Z.L.F.; project administration, Z.L.F. and M.A.L.; funding acquisition, Z.L.F. and M.A.L. All authors have read and agreed to the published version of the manuscript.

Funding: This research was funded by the Chilean National Fund for Scientific and Technological Development (FONDECYT), through the ANID/FONDECYT Regular (grant N° 1221951). Additional funding was provided by the Vicerrectoría de Investigación y Desarrollo (VID) at the Universidad de Chile, under the Programa de Apoyo a Proyectos de Enlace con Concurso Fondecyt Regular VID 2023 (grant N° ENL21/23) and FONDECYT Regular N° 1241485.

Institutional Review Board Statement: Not applicable.

Informed Consent Statement: Not applicable.

Data Availability Statement: The datasets generated and/or analyzed during this study are available from the corresponding author upon reasonable request and available at: Zenodo, https://doi.org/10.5281/zenodo.15045196.

Acknowledgments: We would like to thank the Chilean Ministry of the Environment for making these data available.

Conflicts of Interest: The authors declare no conflicts of interest.

Abbreviations

The following abbreviations are used in this manuscript:

PM	Particulate Matter ($PM_{2.5}$ and PM_{10} refer to PM of diameters less than 2.5 or 10 μm diameter)
SINCA	National Air Quality Information System
MMA	Chilean Ministry of the Environment
ClNAQS	Chilean Air Quality limit levels
WHO	World Health Organisation

References

1. Lelieveld, J.; Pozzer, A.; Pöschl, U.; Fnais, M.; Haines, A.; Münzel, T. Loss of Life Expectancy from Air Pollution Compared to Other Risk Factors: A Worldwide Perspective. *Cardiovasc. Res.* **2020**, *116*, 1910–1917. [CrossRef]
2. World Bank. The Global Health Cost of PM2.5 Air Pollution: A Case for Action Beyond 2021. International Development in Focus 2022. © Washington, DC. Available online: https://shorturl.at/JuFoS (accessed on 10 May 2025).
3. OpenAQ. Open Air Quality Data: The Global Landscape 2024. Available online: https://tinyurl.com/28jxu3tk (accessed on 10 May 2025).
4. World Bank and Institute for Health Metrics and Evaluation. The Cost of Air Pollution: Strengthening the Economic Case for Action 2016. Washington, DC World Bank. Available online: https://tinyurl.com/p272fuee (accessed on 10 May 2025).
5. Riojas-Rodríguez, H.; da Silva, A.S.; Texcalac-Sangrador, J.L.; Moreno-Banda, G.L. Air Pollution Management and Control in Latin America and the Caribbean: Implications for Climate Change. *Rev. Panam. Salud Publica* **2016**, *40*, 150–159. [PubMed]
6. Jorquera, H. Air Quality Management in Chile: Effectiveness of $PM_{2.5}$ Regulations. *Urban Clim.* **2021**, *35*, 100764. [CrossRef]
7. Hartinger, S.M.; Yglesias-González, M.; Blanco-Villafuerte, L.; Palmeiro-Silva, Y.K.; Lescano, A.G.; Stewart-Ibarra, A.; Rojas-Rueda, D.; Melo, O.; Takahashi, B.; Buss, D.; et al. The 2022 South America Report of The Lancet Countdown on Health and Climate Change: Trust the Science. Now That We Know, We Must Act. *Lancet Reg. Health Am.* **2023**, *20*, 100470. [CrossRef] [PubMed]
8. Gouveia, N.; Kephart, J.L.; Dronova, I.; McClure, L.; Granados, J.T.; Betancourt, R.M.; O'Ryan, A.C.; Texcalac-Sangrador, J.L.; Martinez-Folgar, K.; Rodríguez, D.; et al. Ambient Fine Particulate Matter in Latin American Cities: Levels, Population Exposure, and Associated Urban Factors. *Sci. Total Environ.* **2021**, *772*, 145035. [CrossRef] [PubMed]
9. IQAir. World Air Quality Report 2024. Available online: https://www.iqair.com/newsroom/waqr-2024-pr (accessed on 10 May 2025).
10. Lillo, D.; Salazar, C.; Jaime, M.; Chávez, C. Perceptions of Problems and Preferences for Solutions: The Case of Poor Air Quality in Central-Southern Chile. *Energy Sustain. Dev.* **2022**, *66*, 79–91. [CrossRef]
11. Reyes, R.; Schueftan, A.; Ruiz, C.; González, A.D. Controlling Air Pollution in a Context of High Energy Poverty Levels in Southern Chile: Clean Air but Colder Houses? *Energy Policy* **2019**, *124*, 301–311. [CrossRef]
12. Molina, C.; Toro, R.; Morales, R.; Manzano, C.; Leiva-Guzmán, M.A. Particulate Matter in Urban Areas of South-Central Chile Exceeds Air Quality Standards. *Air Qual. Atmos. Health* **2017**, *10*, 653–667. [CrossRef]
13. Huneeus, N.; Urquiza, A.; Gayo, E.; Osses, M.; Arriagada, R.; Valdés, M.; Álamos, N.; Amigo, C.; Arrieta, D.; Basoa, K.; et al. *El Aire que Respiramos: Pasado, Presente y Futuro—Contaminación Atmosférica por $MP_{2.5}$ en el Centro y Sur de Chile*; Centro de Ciencia del Clima y la Resiliencia (CR)2: Santiago, Chile, 2020; 102p, Available online: https://www.cr2.cl/contaminacion/ (accessed on 10 May 2025).
14. Barraza, F.; Lambert, F.; Jorquera, H.; Villalobos, A.M.; Gallardo, L. Temporal Evolution of Main Ambient $PM_{2.5}$ Sources in Santiago, Chile, from 1998 to 2012. *Atmos. Chem. Phys.* **2017**, *17*, 10093–10107. [CrossRef]
15. Gallardo, L.; Barraza, F.; Ceballos, A.; Galleguillos, M.; Huneeus, N.; Lambert, F.; Ibarra, C.; Munizaga, M.; O'Ryan, R.; Osses, M.; et al. Evolution of Air Quality in Santiago: The Role of Mobility and Lessons from the Science–Policy Interface. *Elem. Sci. Anthr.* **2018**, *6*, 38. [CrossRef]
16. Seguel, R.J.; Gallardo, L.; Fleming, Z.L.; Landeros, S. Two Decades of Ozone Standard Exceedances in Santiago de Chile. *Air Qual. Atmos. Health* **2020**, *13*, 593–605. [CrossRef]
17. Seguel, R.J.; Castillo, L.; Opazo, C.; Rojas, N.Y.; Nogueira, T.; Cazorla, M.; Gavidia-Calderón, M.; Gallardo, L.; Garreaud, R.; Carrasco-Escaff, T.; et al. Changes in South American Surface Ozone Trends: Exploring the Influences of Precursors and Extreme Events. *Atmos. Chem. Phys.* **2024**, *24*, 8225–8242. [CrossRef]
18. González-Rojas, C.H.; Leiva-Guzmán, M.A.; Manzano, C.A.; Araya, R.T. Short-Term Air Pollution Events in the Atacama Desert, Chile. *J. S. Am. Earth Sci.* **2021**, *105*, 103010. [CrossRef]
19. Osses, M.; Rojas, N.; Ibarra, C.; Valdebenito, V.; Laengle, I.; Pantoja, N.; Osses, D.; Basoa, K.; Tolvett, S.; Huneeus, N.; et al. High-Resolution Spatial-Distribution Maps of Road Transport Exhaust Emissions in Chile, 1990–2020. *Earth Syst. Sci. Data* **2022**, *14*, 1359–1376. [CrossRef]
20. Alamos, N.; Huneeus, N.; Opazo, M.; Osses, M.; Puja, S.; Pantoja, N.; Denier van der Gon, H.; Schueftan, A.; Reyes, R.; Calvo, R. High-Resolution Inventory of Atmospheric Emissions from Transport, Industrial, Energy, Mining and Residential Activities in Chile. *Earth Syst. Sci. Data* **2022**, *14*, 361–379. [CrossRef]
21. Olivares, G.; Gallardo, L.; Langner, J.; Aarhus, B. Regional Dispersion of Oxidized Sulfur in Central Chile. *Atmos. Environ.* **2002**, *36*, 3819–3828. [CrossRef]
22. OECD. *OECD Environmental Performance Reviews: Chile 2024*; OECD Publishing: Paris, France, 2024. [CrossRef]
23. Toro, R.A.; Campos, C.; Molina, C.; Morales, S.R.G.E.; Leiva-Guzmán, M.A. Accuracy and Reliability of Chile's National Air Quality Information System for Measuring Particulate Matter: Beta Attenuation Monitoring Issue. *Environ. Int.* **2015**, *82*, 101–109. [CrossRef]

24. Quinteros, M.E.; Blanco, E.; Sanabria, J.; Rozas-Díaz, F.; Blázquez, C.; Ayala, S.; Cárdenas, J.P.; Stone, E.A.; Sybesma, K.; Delgado-Saborit, J.M.; et al. Spatio-Temporal Distribution of Particulate Matter and Wood-Smoke Tracers in Temuco, Chile: A City Heavily Impacted by Residential Wood-Burning. *Atmos. Environ.* **2023**, *294*, 119529. [CrossRef]
25. Manzano, C.A.; Jácome, M.; Syn, T.; Molina, C.; Toro Araya, R.; Leiva-Guzmán, M.A. Local Air Quality Issues and Research Priorities through the Lenses of Chilean Experts: An Ontological Analysis. *Integr. Environ. Assess. Manag.* **2021**, *17*, 273–281. [CrossRef]
26. Villacura, L.; Sánchez, L.F.; Catalán, F.; Toro-Araya, R.; Leiva-Guzmán, M.A. An Overview of Air Pollution Research in Chile: Bibliometric Analysis and Scoping Review, Challenges and Future Directions. *Heliyon* **2024**, *10*, e25431. [CrossRef]
27. Gallardo, L.; Olivares, G.; Langner, J.; Aarhus, B. Coastal Lows and Sulfur Air Pollution in Central Chile. *Atmos. Environ.* **2002**, *36*, 3829–3841. [CrossRef]
28. MMA. *Decreto 39: Aprueba Reglamento para la Dictación de Planes de Prevención y de Descontaminación*; Ministerio del Medio Ambiente: Santiago, Chile, 2013; Available online: https://www.bcn.cl/leychile/navegar?idnorma=1053037&idparte=&idversion= (accessed on 10 May 2025).
29. Zanetta-Colombo, N.C.; Fleming, Z.L.; Gayo, E.M.; Manzano, C.A.; Panagi, M.; Valdés, J.; Siegmund, A. Impact of Mining on the Metal Content of Dust in Indigenous Villages of Northern Chile. *Environ. Int.* **2022**, *169*, 107490. [CrossRef] [PubMed]
30. García, D.; Tapia, J.; Aguilera, J.; Vega, C.; Zúñiga, P.; Lavín, P.; Rojas, L.; Valdés, J. Contamination of Urban Soils in a Historical Mining Town of Northern Chile. *Environ. Earth Sci.* **2024**, *83*, 11445. [CrossRef]
31. Toro, R.; Claramunt, T.; González, F.; Ávila, S.; Leiva-Guzmán, M.A. Long-Term Assessment and Acute Air Pollution Events in a Mega-Industrial Area in Central Chile. *Urban Clim.* **2024**, *55*, 101880. [CrossRef]
32. Seguel, R.J.; Garreaud, R.; Muñoz, R.; Bozkurt, D.; Gallardo, L.; Opazo, C.; Jorquera, H.; Castillo, L.; Menares, C. Volatile Organic Compounds Measured by Proton Transfer Reaction Mass Spectrometry over the Complex Terrain of Quintero Bay, Central Chile. *Environ. Pollut.* **2023**, *330*, 121759. [CrossRef] [PubMed]
33. Seguel, R.J.; Gallardo, L.; Osses, M.; Rojas, N.Y.; Nogueira, T.; Menares, C.; de Fatima Andrade, M.; Belalcázar, L.C.; Carrasco, P.; Eskes, H.; et al. Photochemical Sensitivity to Emissions and Local Meteorology in Bogotá, Santiago, and São Paulo: An Analysis of the Initial COVID-19 Lockdowns. *Elem. Sci. Anthr.* **2022**, *10*, 00044. [CrossRef]
34. Schreck, E.; Le Goff, L.; Calas, A.; Fleming, Z.L.; Bosch, C.; Yettou, A.; Mesas, M.; Martínez-Lladó, X.; Vallejos-Romero, A.; Blot, F.; et al. An Interdisciplinary Approach for Air Quality Assessment: Biomonitoring Using Tillandsia bergeri and Risk Perceptions in the Environmentally Sacrificed Province of Chacabuco, Chile. *Environ. Geochem. Health* **2025**, *47*, 99. [CrossRef]
35. Solis, R.; Toro, R.; Gomez, L.; Vélez, A.M.; López, M.; Fleming, Z.L.; Fierro, N.; Leiva, M. Long-Term Airborne Particle Pollution Assessment in the City of Coyhaique, Patagonia, Chile. *Urban Clim.* **2022**, *43*, 101144. [CrossRef]
36. Mardones, C. Contribution of the Carbon Tax, Phase-Out of Thermoelectric Power Plants, and Renewable Energy Subsidies for the Decarbonization of Chile—A CGE Model and Microsimulations Approach. *J. Environ. Manag.* **2024**, *352*, 120017. [CrossRef]
37. Rueda-Holgado, F.; Palomo-Marín, M.R.; Calvo-Blázquez, L.; Cereceda-Balic, F.; Pinilla-Gil, E. Fractionation of Trace Elements in Total Atmospheric Deposition by Filtrating-Bulk Passive Sampling. *Talanta* **2014**, *125*, 125–130. [CrossRef]
38. Gayo, E.M.; Muñoz, A.A.; Maldonado, A.; Lavergne, C.; François, J.P.; Rodríguez, D.; Klock-Barría, K.; Sheppard, P.R.; Aguilera-Betti, I.; Alonso-Hernández, C.; et al. *A* Cross-Cutting Approach for Relating Anthropocene, Environmental Injustice and Sacrifice Zones. *Earth's Future* **2022**, *10*, e2021EF002217. [CrossRef]
39. Tapia-Gatica, J.; González-Miranda, I.; Salgado, E.; Bravo, M.A.; Tessini, C.; Dovletyarova, E.A.; Paltseva, A.A.; Neaman, A. Advanced Determination of the Spatial Gradient of Human Health Risk and Ecological Risk from Exposure to As, Cu, Pb, and Zn in Soils near the Ventanas Industrial Complex (Puchuncaví, Chile). *Environ. Pollut.* **2020**, *258*, 113488. [CrossRef] [PubMed]
40. Cereceda-Balic, F.; Gala-Morales, M.; Palomo-Marín, R.; Fadic, X.; Vidal, V.; Funes, M.; Rueda-Holgado, F.; Pinilla-Gil, E. Spatial Distribution, Sources, and Risk Assessment of Major Ions and Trace Elements in Rainwater at Puchuncaví Valley, Chile: The Impact of Industrial Activities. *Atmos. Pollut. Res.* **2020**, *11*, 99–109. [CrossRef]
41. Gorena, T.; Fadic, X.; Cereceda-Balic, F. Cupressus macrocarpa Leaves for Biomonitoring the Environmental Impact of an Industrial Complex: The Case of Puchuncaví–Ventanas in Chile. *Chemosphere* **2020**, *260*, 127521. [CrossRef]
42. Muñoz, A.A.; Klock-Barría, K.; Sheppard, P.R.; Aguilera-Betti, I.; Toledo-Guerrero, I.; Christie, D.A.; Gorena, T.; Gallardo, L.; González-Reyes, Á.; Lara, A.; et al. Multidecadal Environmental Pollution in a Mega-Industrial Area in Central Chile Registered by Tree Rings. *Sci. Total Environ.* **2019**, *696*, 133915. [CrossRef] [PubMed]
43. Tume, P.; Acevedo, V.; Roca, N.; Ferraro, F.X.; Bech, J. Potentially Toxic Elements Concentrations in Schoolyard Soils in the City of Coronel, Chile. *Environ. Geochem. Health* **2022**, *44*, 1521–1535. [CrossRef]
44. Hamed, K.H.; Rao, A.R. A Modified Mann–Kendall Trend Test for Autocorrelated Data. *J. Hydrol.* **1998**, *204*, 182–196. [CrossRef]
45. Van der Walt, S.; Colbert, S.C.; Varoquaux, G. The NumPy Array: A Structure for Efficient Numerical Computation. *Comput. Sci. Eng.* **2011**, *13*, 22–30. [CrossRef]
46. McKinney, W. Data Structures for Statistical Computing in Python. In Proceedings of the 9th Python in Science Conference, Austin, TX, USA, 28 June–3 July 2010; van der Walt, S., Millman, J., Eds.; SciPy: Austin, TX, USA, 2010; pp. 51–56.

47. Hunter, J.D. Matplotlib: A 2D Graphics Environment. *Comput. Sci. Eng.* **2007**, *9*, 90–95. [CrossRef]
48. Harris, C.R.; Millman, K.J.; van der Walt, S.J.; Gommers, R.; Virtanen, P.; Cournapeau, D.; Wieser, E.; Taylor, J.; Berg, S.; Smith, N.J.; et al. Array Programming with NumPy. *Nature* **2020**, *585*, 357–362. [CrossRef]
49. Reitz, K. Requests: HTTP for Humans. 2013. Available online: https://docs.python-requests.org/ (accessed on 10 May 2025).
50. Richardson, L. Beautiful Soup Documentation. 2017. Available online: https://tinyurl.com/y64ubcw8 (accessed on 10 May 2025).
51. Jordahl, K.; Wasserman, J.; McBride, J.; Wilson, J.; Arribas-Bel, D.; Gerard, J. GeoPandas: Python Tools for Geographic Data [Computer software]. 2020. Available online: https://github.com/geopandas/geopandas (accessed on 10 May 2025).
52. Gillies, S. Shapely: Manipulation and Analysis of Geometric Objects in the Cartesian Plane [Computer software]. 2007. Available online: https://github.com/shapely/shapely (accessed on 10 May 2025).
53. Hussain, M.; Mahmud, I.; Bellouin, N. pyMannKendall: A Python Package for Nonparametric Mann–Kendall Family of Trend Tests. *J. Open Source Softw.* **2019**, *4*, 1556. [CrossRef]
54. World Health Organization. *WHO Global Air Quality Guidelines: Particulate Matter (PM2.5 and PM10), Ozone, Nitrogen Dioxide, Sulfur Dioxide and Carbon Monoxide*; World Health Organization: Geneva, Switzerland, 2021; Available online: https://www.who.int/publications/i/item/9789240034228 (accessed on 10 May 2025).
55. MMA. *Decreto 40: Establece Norma Primaria de Calidad de aire Para Dióxido de Nitrógeno (NO2)*; Ministerio del Medio Ambiente: Santiago, Chile, 2024; Available online: https://www.bcn.cl/leychile/navegar?idNorma=1206820 (accessed on 10 May 2025).
56. MMA. *Decreto 104: Establece Norma Primaria de Calidad de aire para Dióxido de Azufre (SO2)*; Ministerio del Medio Ambiente: Santiago, Chile, 2019; Available online: https://www.bcn.cl/leychile/navegar?idNorma=1131641 (accessed on 10 May 2025).
57. MMA. *Decreto 115: Establece Norma Primaria de Calidad de aire Para Monóxido de Carbono (CO)*; Ministerio del Medio Ambiente: Santiago, Chile, 2022; under revision 2025; Available online: https://www.bcn.cl/leychile/navegar?idNorma=202437 (accessed on 10 May 2025).
58. *Decreto 112: Establece Norma Primaria de Calidad de Aire Para Ozono (O_3)*; Ministerio del Medio Ambiente: Santiago, Chile, 2003; under revision 2025; Available online: https://www.bcn.cl/leychile/navegar?idNorma=208198 (accessed on 10 May 2025).
59. *Decreto 12: Establece Norma Primaria de Calidad de Aire Para Material Particulado Respirable (MP10)*; Ministerio del Medio Ambiente: Santiago, Chile, 2022; Available online: https://www.bcn.cl/leychile/navegar?idNorma=1176988 (accessed on 10 May 2025).
60. MMA. *Decreto 12: Establece Norma Primaria de Calidad de Aire Para Material Particulado Fino Respirable (MP2.5)*; Ministerio del Medio Ambiente: Santiago, Chile, 2011; under revision 2024–2025; Available online: https://www.bcn.cl/leychile/navegar?idNorma=1025202 (accessed on 10 May 2025).

Disclaimer/Publisher's Note: The statements, opinions and data contained in all publications are solely those of the individual author(s) and contributor(s) and not of MDPI and/or the editor(s). MDPI and/or the editor(s) disclaim responsibility for any injury to people or property resulting from any ideas, methods, instructions or products referred to in the content.